

INVESTIGATION OF CONSTRUCTION PARAMETERS INFLUENCE IN AEROELASTIC MODAL EVOLUTION CURVE USING THE ROGER METHOD AND STRIP MODELS.

Carlos Eduardo de Souza, carloseduardos@iae.cta.br

André Balbi Aguiar, andre_balbi@hotmail.com

Roberto Gil Annes da Silva, rasilva@iae.cta.br

Adolfo Gomes Marto, agmarto@iae.cta.br

Instituto de Aeronáutica e Espaço, Praça Marechal Eduardo Gomes, 50 - Campus do CTA - Vila das Acácias, CEP 12228-904 - São José dos Campos - SP - Brasil

Abstract. *The influence of ply orientation in the aeroelastic modal evolution curve of a laminated composite wing is investigated. A state space flutter stability analysis is performed based in a finite state aerodynamic approximation. The unsteady aerodynamic theory is based in the two dimensional Theodorsen's solution, using strip approach for a three dimensional aerodynamic modeling. The structural information is obtained from modal analysis employing the Finite Element Method. The internal spars are modeled with equivalent beam elements and the surface with shells. Results show a strong influence in the flutter speed and modal behavior. The sensitivity aeroelastic investigation will allow the design and fabrication of representative experimental wing models. This work is a first step in a more complete investigation which will include, in the near future, wind-tunnel experimental analysis to validate the numerical models.*

Keywords: *Aeroelastic stability analysis; Laminated composite wing; ply orientation; Roger method; Strip models*

1. INTRODUCTION

The aeroelastic stability analysis is an important step in aircraft design. In the last decades, with the increasing flexibility of aeronautical structures, the response analysis became also important in the design and certification process. Besides that, with the constant improvement of control system hardware and automatic control methods, mostly due to the advent of Unmanned Aircraft, the inclusion of control systems in the aeroelastic analysis became more a must than a need.

The State Space Aeroelastic modeling allows not only the aeroelastic stability analysis but also the response and flight dynamic analysis, with the inclusion of control laws in the state equations (Roger, 1977). The finite state aerodynamic modeling is an approach based on the transformation from the frequency domain defined aerodynamic (e.g. Theodorsen) to a time domain state space representation. Due to that, this method has been chosen to be implemented as a tool for a multidisciplinary research in the development and analysis of highly flexible wings. The method implementation passes through different phases before reaching the point where it can be used to analyze advanced aerodynamic and structural models. After having the method working with typical section, with simplified aerodynamic and structural information, the strip method has been implemented.

One of the goals is to study the behavior of laminated composite wings. Laminated composite material is already largely employed in aeronautical construction. However, there are still plenty of questions to be answered, due, mainly, to the almost infinite possibility of methods, arrangements and types of material that can be combined. This is, indeed, what makes the composite material so attractive to the designer. The use of composite material in optimized structures may lead to highly flexible structures with nonlinear behavior. The influence of all the parameters in the aeroelastic behavior of wings aren't still well addressed. The aeroelastic tailoring will be the next step of a research in this area.

Studies of composite flat plates and shallow shells are presented in Bismarck-Nasr (1999), and some results are presented for panel-like structures. Works in the eighties (Shirk et al., 1986) and nineties presented studies of wings with a the structural model as a box, with composite laminated material around all walls. Cesnik et al. (1996) is an example of work where the structural model is based on a nonlinear geometric beam analysis. In the work of da Rocha (1999) a simple flat plate composite laminated wing has been analyzed, showing the influence of ply orientation in the velocity of the instability point. These works are related to aeroelastic tailoring, what can be defined as the use of the design flexibility of composite material to achieve a desired global behavior (Rehfield, 2002).

In this paper, the application of Roger approximation method for time domain unsteady aerodynamic modeling combined with a strip theory to a laminated composite wing is presented. The proposal here is to work with structural and aerodynamic models of average complexity. The structural information, basically the modal information, is obtained through a Finite Element Method (FEM) analysis, using MSC/NASTRAN (MSC, 2001). The flutter analysis here performed is an aeroelastic stability analysis, where an state space aeroelastic matrix is assembled and its eigenvalues and eigenvectors are calculated for a range of velocities. Velocity-damping-frequency (v-g-f) curves are obtained, allowing the comparison between models with different lamination sequences.

This work represents a first step in the study of complex aerodynamic systems made of composite material. The wings here analyzed are preliminary models for the definition of scaled models to be constructed in order to validate the theoretical analysis. The results presented here show a big influence of laminated configurations in the flutter speed and in the aeroelastic modal evolution. Further work addressing the parameters identification will be made along with modeling construction.

2. STATE SPACE AEROELASTIC MODEL

The present formulation is based on the model of an aeroelastic system using modal superposition :

$$m_e \ddot{\eta}_e(t) + b_e \dot{\eta}_e(t) + k_e \eta_e(t) = \Phi_e^T L_e(t, x_e(t), \dot{x}_e(t), \ddot{x}_e(t)). \quad (1)$$

Here m_e , b_e , k_e are the generalized mass, damping, and stiffness matrices; Φ_e is the modal matrix; $\eta_e(t)$ is the generalized coordinate vector; $x_e(t) = \Phi_e \eta_e(t)$ is the original coordinate vector; and $L_e(t, x_e, \dot{x}_e, \ddot{x}_e)$ is the aerodynamic loading vector. Note that the subscript $(\cdot)_e$ denotes quantities defined in terms of a structural coordinate system.

The aerodynamic influence coefficients are computed based on boundary conditions defined at aerodynamic control points. However, the displacement vector for the boundary conditions computation is oftenly written in FEM model nodal coordinates. Due to that, there is a need for a displacement transformation between the aerodynamic model and the finite element model (FEM). In simple structures, all the FEM grid points can be used. However, in more complex structures, the selection of only a few representative points is necessary, lowering the aeroelastic model order. In the present work, a list of representative grid points of the finite element model is used. These points are those which allows a good representation of the modal displacement for all the modes taken into account.

A procedure based in an interpolation using surface splines has been implemented accordingly with theories presented in the ZAERO theoretical manual (ZONA Technology, 2007). Two methods were implemented: the Infinite Plate Spline Method (IPS), which works with both structural and aerodynamic models in the same plane (Harder and Desmarais, 1972); and the Thin-Plate Spline Method (TPS), which allows for points out of plane in the structural model (see Duchon, 1976).

Mathematically speaking, for the representation of the physical coordinates in another points, the following transformation is used:

$$\mathbf{x}_a = \mathbf{G}_s \mathbf{x}_e. \quad (2)$$

where \mathbf{G}_s is a transformation matrix, given by the spline transformation presented by Harder and Desmarais (1972). In the same manner, the modal displacements can be written using the same conversion type through interpolation. In this case, the transformation is applied to each modal matrix:

$$\phi_a = \mathbf{G}_s \phi_e. \quad (3)$$

With this transformation, it is possible to assembly the aeroelastic system in the frequency space, and work only with generalized matrices:

$$\tilde{\mathbf{M}}_e \ddot{\eta}_e(t) + \tilde{\mathbf{K}}_e \eta_e(t) = \Phi_a^T \mathbf{L}_a(t). \quad (4)$$

where the generalized structural matrices area calculated as $\tilde{\mathbf{M}}_e = \phi_e^T \mathbf{M}_e \phi_e$ and $\tilde{\mathbf{K}}_e = \phi_e^T \mathbf{K}_e \phi_e$. The final analysis dimension in both sides of Eq. (4) will be the number of modes taken into account. The code implemented uses the modal information obtained from the analysis of a wing FEM. The only used information are: the grid points positions, the modal displacements and the frequency for each model. The term L_e can be represented in the frequency domain as follows:

$$\mathbf{L}_e(k, x_a) = \mathbf{G}_s^T \mathbf{L}_a(k, x_a) = \mathbf{q}_d \mathbf{G}_s^T \mathbf{A}(k) \mathbf{x}_a. \quad (5)$$

The subscript $(\cdot)_a$ denotes that the quantity is related to the aerodynamic coordinate system obtained from the discretization of the lifting surface or body. Note that q_d is the dynamic pressure, and $k = \omega b/U$ is the so-called reduced frequency, where ω is the harmonic frequency, U is the free stream velocity, and b is the reference semi-chord. The aerodynamic influence coefficient matrix $\mathbf{A}(k)$ is a function of the reduced frequency (only incompressible flow is considered here). Since there are two coordinate systems involved it is necessary to interconnect them through a transformation, which is given by the matrix \mathbf{G}_s , i.e., $\mathbf{x}_a = \mathbf{G}_s \mathbf{x}_e$. Usually, this matrix is associated with a transformation using surface splines Harder and Desmarais (1972). Therefore, equation (1) may be rewritten as

$$\begin{aligned} m_e \ddot{\eta}_e(t) + b_e \dot{\eta}_e(t) + k_e \eta_e(t) &= \mathbf{q}_d \Phi_a^T \mathbf{A}(k) \mathbf{G}_s x_e(t) \\ &= \mathbf{q}_d \Phi_a^T \mathbf{A}(k) \mathbf{G}_s \Phi_e \eta_e(t) \\ &= \mathbf{q}_d \Phi_a^T \mathbf{A}(k) \Phi_e \eta_e(t) \\ &= \mathbf{q}_d \mathbf{A}^*(k) \eta_e(t). \end{aligned} \quad (6)$$

Note that $\Phi_a = \mathbf{G}_s \Phi_e$ is the modal matrix related to the aerodynamic coordinate system.

The usual procedure to solve aeroelastic problems is based on the eigensolution of equation (6), varying either the reduced frequency or the velocity to obtain the aerodynamic loads. The most common method employed is the so-called k method, which is based on the assumption that all motion is purely harmonic, and that the aerodynamic matrix can be added to the mass matrix. Its main disadvantage is that the solution is only physically valid for zero damping or at the prescribed structural damping g_0 . Another usual alternative is the p - k method (Hassig, 1971), where only the aerodynamic loads are assumed to depend upon pure harmonic motion. Because this is an iterative method, it is more computationally intensive than the k method. On the other hand, the aeroelastic damping evolutions with velocity are at least qualitatively representative of the real system. A more detailed discussion of the mathematical procedures of these methods can be found in the work of da Silva (1994) and Hassig (1971).

The method developed here can be classified as a p method, implying that everything is calculated assuming arbitrary motion. It consists in approximating a set of aerodynamic influence coefficient matrices, $\mathbf{A}^*(k_m)$, $m = 1, \dots, m_k$, obtained for m_k values of reduced frequencies, by a representative function of the Laplace variable s . This function is known as a Padé polynomial (Vepa, 1977), and have up to second order terms in the Laplace variable s , as well as a series of poles, that is,

$$\mathbf{A}^*(k) \rightarrow \mathbf{A}^*(s) \simeq \mathbf{A}_{ap}^*(s), \quad (7)$$

where

$$\mathbf{A}_{ap}^*(s) = \mathbf{A}_0^* + \mathbf{A}_1^* s \left(\frac{b}{U} \right) + \mathbf{A}_2^* s^2 \left(\frac{b}{U} \right)^2 + \sum_{n=1}^{n_{lag}} \frac{s \mathbf{A}_{n+2}^*}{s + (U/b)} \beta_n. \quad (8)$$

It should be noted that $ik = sb/U$ on the imaginary axis. The β_n are called lag parameters since they are physically related to the inherent lag present between motion and load in unsteady phenomena. The values of these parameters can be obtained either by optimization procedures or by user's experience. The coefficient matrices \mathbf{A}_j^* , $j = 1, \dots, 2 + n_{lag}$, of Padé polynomial are obtained using the least-square method (applied for complex numbers) in order to fit the set of tabulated matrices $\mathbf{A}^*(k_m)$. More details of this procedure may be found in the works of da Silva (1994).

Once the above rational approximation has been obtained, one can write equation (6) as

$$m_e s^2 \eta_e(s) + b_e s \eta_e(s) + k_e \eta_e(s) = q_d \mathbf{A}_{ap}^*(s) \eta_e(s). \quad (9)$$

In order to obtain a state-space formulation it is necessary to apply the inverse Laplace transform to equation (9). If one does this and uses expression (8), the result is given by

$$\begin{aligned} m_e s^2 \eta_e(s) + b_e s \eta_e(s) + k_e \eta_e(s) &= q_d \mathbf{A}_0^* \eta_e(t) + q_d \mathbf{A}_1^* \dot{\eta}_e(t) \left(\frac{b}{U} \right) + q_d \mathbf{A}_2^* \ddot{\eta}_e(t) \left(\frac{b}{U} \right)^2 \\ &+ q_d \sum_{n=1}^{n_{lag}} \mathbf{A}_{n+2}^* \eta_{lag}(t)_n. \end{aligned} \quad (10)$$

The states $\eta_{lag}(t)_n$ are the so-called aerodynamically augmented or lag states, and they appear because of the rational form of the pole series. They may be obtained applying the convolution theorem to the product of functions

$$\frac{\mathbf{A}_{n+2}^*}{s + (U/b)} s \eta_e(s), \quad (11)$$

where the following inverse Laplace transforms are known:

$$\mathcal{L}^{-1} [s \eta_e(s)] = \dot{\eta}_e(t), \quad \mathcal{L}^{-1} \left[\frac{\mathbf{A}_{n+2}^*}{s + (U/b)} \beta_n \right] = \mathbf{A}_{n+2}^* e^{-(U/b) \beta_n t}. \quad (12)$$

Therefore,

$$\eta_{lag}(t)_n = \int_0^t \dot{\eta}_e(\tau) e^{-(U/b) \beta_n (t - \tau)} d\tau. \quad (13)$$

Differentiation of equation (13) gives a set of ordinary differential equations for the lag states, which can be included in the set of equations of the aeroelastic system:

$$\dot{\eta}_{lag}(t)_n = \dot{\eta}_e(t) - \frac{b}{U} \beta_n \eta_{lag}(t)_n. \quad (14)$$

The aeroelastic system can then be represented by a unique state matrix, with only the free stream velocity as argument:

$$\dot{\xi}(t) = \mathcal{A}(U)\xi(t). \quad (15)$$

The state matrix $\mathcal{A}(U)$ is given by

$$\mathcal{A}(U) = \begin{bmatrix} -\tilde{\mathbf{M}}^{-1}\tilde{\mathbf{B}} & -\tilde{\mathbf{M}}^{-1}\tilde{\mathbf{K}} & \tilde{\mathbf{M}}^{-1}\tilde{\mathbf{A}}_3 & \cdots & \tilde{\mathbf{M}}^{-1}\tilde{\mathbf{A}}_{n+2} \\ \mathbf{I} & 0 & 0 & \cdots & 0 \\ \mathbf{I} & 0 & -\left(\frac{U}{b}\right)\beta_1\mathbf{I} & \cdots & 0 \\ \vdots & \vdots & \vdots & \ddots & \vdots \\ \mathbf{I} & 0 & 0 & \cdots & -\left(\frac{U}{b}\right)\beta_n\mathbf{I} \end{bmatrix}, \quad (16)$$

The state matrix $\mathcal{A}(U)$ has the following matrices in its definition:

$$\begin{aligned} \tilde{\mathbf{M}} &= \mathbf{M}_e - q_d \left(\frac{b}{U}\right)^2 \mathbf{A}_2^*, & \tilde{\mathbf{B}} &= \mathbf{B}_e - q_d \left(\frac{b}{U}\right)^1 \mathbf{A}_1^*, \\ \tilde{\mathbf{K}} &= \mathbf{K}_e - q_d, & \tilde{\mathbf{A}}_{n+2} &= q_d \mathbf{A}_{n+2}^*. \end{aligned} \quad (17)$$

The definition of \mathbf{M}_e , \mathbf{B}_e , \mathbf{K}_e and q_D can be found in [da Silva \(1994\)](#).

In the strip theory, a tri-dimensional model is analyzed through known bi-dimensional methods. The wing is divided into different typical sections along its span. The influence coefficients matrix is assembled as a combination of all of these sections. This theory is limited to cases where the tridimensional effects can be ignored, such as long span wings. In Fig. 1, an example of a model with 3 different types of section is shown.

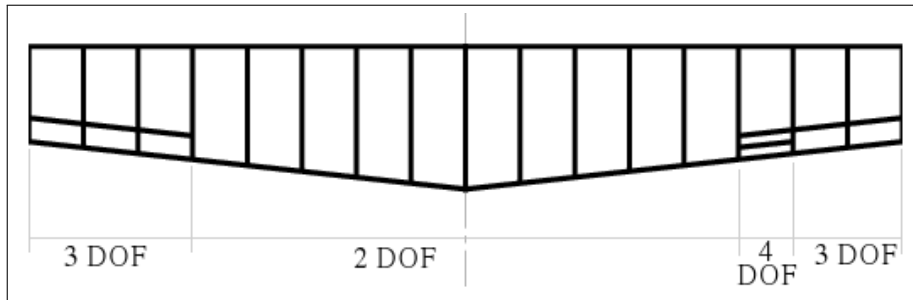


Figure 1. Strip theory aerodynamic model of a wing with 3 different types of typical sections (after [da Silva, 1994](#)).

Each strip has a finite width, from which it is possible to calculate the loading L_i along all the strip span, dy_i , doing $L_i = \bar{l}dy_i$. The loading obtained through Theodorsen's theory is given as a function of unit span, and only the motions related to the degrees of freedom of each strip are taken into account. As an example for a 2 DOF strip, its loading is given by:

$$\begin{Bmatrix} -(\bar{l}b)_i \\ (\bar{m}_y)_i \end{Bmatrix} = \pi\rho b_i^4 \omega^2 \begin{bmatrix} l_h & l_\alpha \\ m_h & m_\alpha \end{bmatrix} \begin{Bmatrix} (\bar{h}/b)_i \\ (\bar{\alpha})_i \end{Bmatrix} \Rightarrow \bar{\mathbf{P}}_i = \mathbf{A}(ik)_i \bar{\mathbf{x}}_i. \quad (18)$$

For a complete wing, with N strips along its span, the loading is given by:

$$\begin{Bmatrix} \bar{\mathbf{P}}_1 \\ \bar{\mathbf{P}}_2 \\ \bar{\mathbf{P}}_3 \\ \vdots \\ \bar{\mathbf{P}}_N \end{Bmatrix} = \pi\rho \begin{bmatrix} b_1^4 \mathbf{A}_1(ik) & 0 & \cdots & \cdots & 0 \\ 0 & b_2^4 \mathbf{A}_2(ik) & \cdots & \cdots & 0 \\ 0 & 0 & b_3^4 \mathbf{A}_3(ik) & \cdots & 0 \\ \vdots & \vdots & \vdots & \ddots & 0 \\ 0 & 0 & 0 & \cdots & b_N^4 \mathbf{A}_N(ik) \end{bmatrix} \begin{Bmatrix} \bar{\mathbf{x}}_1 \\ \bar{\mathbf{x}}_2 \\ \bar{\mathbf{x}}_3 \\ \vdots \\ \bar{\mathbf{x}}_N \end{Bmatrix} \quad (19)$$

The above global influence matrix has a block diagonal structure, indicating that there is no aerodynamic coupling between each strip. The reduced frequency varies from strip to strip since it depends on each chord. However, these local

reduced frequencies can be written as a function of a reference reduced frequency k_{ref} , properly scaling it by the local semi-chord length divided by the reference semi-chord b_{ref} :

$$k_{ref} = \frac{\omega b_{ref}}{U} \quad \Rightarrow \quad k_i = k_{ref} \left(\frac{b_i}{b_{ref}} \right) \quad (20)$$

This procedure guarantees that the reduced frequency will be the same along the span:

$$\frac{k_1 U}{b_1} = \frac{k_2 U}{b_2} = \frac{k_3 U}{b_3} = \dots = \frac{k_N U}{b_N} = \omega \quad (21)$$

In the Roger method, a set reduced frequency dependent aerodynamic influence coefficients matrix is defined for the approximation procedure, based on a least square method to approximate each its elements individually. Each scalar coefficient of the approximated matrix is calculated as:

$$a_{ap}^{ij}(\imath k_m) = a_0^{ij} + a_1^{ij} \imath k_m - a_2^{ij} k_m^2 + \sum_{n=1}^{nlag} \frac{\imath k_m a_{n+2}^{ij}}{\imath k_m + \beta_{n+2}}, \quad (22)$$

where i and j are the indexes for the position inside $\overline{\mathbf{A}}$, \imath is the imaginary operator, k_m is the m^{th} reduced frequency and $nlag$ is the number of lag terms. In vectorial form, $a_{ap}^{ij}(\imath k_m) = \mathbf{R}(\imath k_m) \mathbf{a}^{ij}$, and the final form to the determination to the a_n^{ij} coefficients is given by

$$\mathbf{a}^{ij} = \left(\mathbf{F}^T \overline{\mathbf{F}} + \overline{\mathbf{F}}^T \mathbf{F} \right)^{-1} \left(\overline{\mathbf{F}}^T \overline{\mathbf{A}}_t^{ij} + \mathbf{F}^T \mathbf{A}_t^{ij} \right), \quad (23)$$

where

$$\mathbf{F} = \left\{ \mathbf{R}(\imath k_1) \quad \mathbf{R}(\imath k_2) \quad \dots \quad \mathbf{R}(\imath k_{mk}) \right\}^T \quad \mathbf{A}_t^{ij} = \left\{ a_t(\imath k_1) \quad a_t(\imath k_2) \quad \dots \quad a_t(\imath k_{mk}) \right\}^T \quad (24)$$

The flutter problem solution consists in solving a series of eigenvalue problems of the matrix \mathcal{A} for a list of velocities. The following procedure is employed to assembly the influence coefficients matrix:

1. assembly of structural matrices;
2. looping in the reference reduced frequency:
 - (a) previous calculation of the Theodorsen matrix at each frequency, for late use;
3. assembly of the approximated matrix:
 - (a) assembly of \mathbf{F} (eq. 24);
 - (b) calculation of the term $\left(\mathbf{F}^T \overline{\mathbf{F}} + \overline{\mathbf{F}}^T \mathbf{F} \right)^{-1}$;
 - (c) looping in the terms of the approximated matrix to obtain the vector \mathbf{a}^{ij} ;
 - (d) save the matrix for a later use;
4. looping in the velocities list:
 - (a) assembly of \mathcal{A} (16);
 - (b) calculation of \mathcal{A} eigenvalues for each v_i .

3. MODEL DESCRIPTION

The wing model consists of a NACA0012 profile with a 4.5 m semispan, a root chord of 1.5m and a tip chord of 1.0 m. There are three ribs, one at the root, other at the tip, and another at 2.5 m from root, where the aileron area begins. The main spar is located at 40% of the chord, and the rear spar at 80% (see Fig. 2).

The finite element model is a 3D model, with plate elements for the modeling the external surfaces, ribs, rear spar and aileron, and beam elements for the main spar. The skin was modeled with composite layered material, with orthotropic properties. The NASTRAN element types are CQUAD4 for plates a CBEAM for the beams.

In actual wings the main spar has a different layup in relation to the wing skin. Besides that, many construction details modify its properties, such as holes and attached hardware. These details would increase the complexity of the FEM model. So, a equivalent isotropic beam property has been established for the main spar.

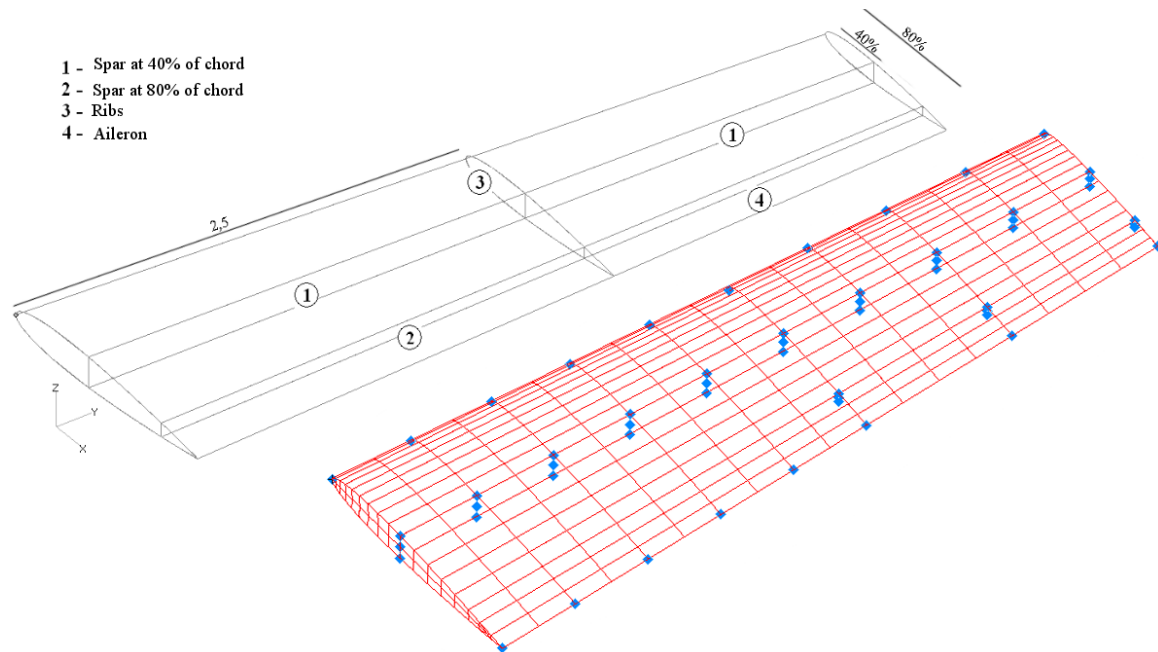


Figure 2. Above: wing model; below: FEM model with selected grid points.

To define the equivalent property, the main spar has been modeled as a beam alone, with a $[0/90]_{10S}$ stacking sequence, using properties of fiberglass fabric, 0.11 mm thick at each layer. The middle layer is a foam core H60, 12 mm thick. The spar caps were modeled with the same stacking sequence, but with carbon fiber properties. A force of 100N has been applied to the spar tip, and the maximum deflection was used to define the cross section properties of equivalent I type 2024 aluminum beam.

Six different types of lamination were considered in this first approach for the wing skin structural model. The lamination is a simple combination of single orthotropic layers, with properties obtained from Reddy (1997) and commercial references. These properties are listed in Table 1 below. The material properties were defined independently for each layer. Another option would be the use of the classical lamination theory, in which a prior definition of the equivalent elastic coefficients are made by a summation of properties of each individual layer (Jones, 1999, Reddy, 1997). This will be implemented in a next step. The aileron is attached to the wing by the use of RBE2 constraints and CELAS2 spring elements, set to 30kNm, in the rotation degree of freedom.

Table 1. Material properties.

	Gr-Ep	Gl-Ep	Foam H60
E1 [Gpa]	137.9	53.78	0.0056
E2/3 [Gpa]	8.9363	17.93	0.0056
G23 [Gpa]	6.21	3.44	0.022
G13/12[Gpa]	7.1	8.96	0.022
v23 [Gpa]	0.49	0.34	0.027
v13/12 [Gpa]	0.3	0.25	0.027
Dens.[kg/m ³]	1700.0	2100.0	60.0

Table 2. Stacking sequence.

Layer	Layup
1	$[0_5C0_5]_T$
2	$[0/45/0/45/0/C/0/45/0/45/0]_T$
3	$[0/90/0/90/0/C/0/90/0/90/0]_T$
4	$[0/45/0/90/0/C/0/90/0/45/0]_T$
5	$[30/45/0/45/0/C/0/45/0/45/30]_T$
6	$[30/-30/0/45/0/C/0/45/0/-30/30]_T$

C: core.

The normal modes for each model are identified in the table 3. This identification is important to include only the significative modes in the analysis. In a more complex problem, a detailed verification should be made, in order to identify clearly the normal modes and its influence in the aeroelastic behavior. In this case, the aileron mode is around 21 Hz for all models. The total mass is 37.45 kg, and is constant also for all models, since the material quantity and type is the same.

In Table 3, the modes marked with an 'x' indicates the modes that are not considered in the present analysis. This modes are local modes, with shell bending. The analysis of these local bending are out of scope of the present work, but must be addressed in future, to verify if there is a possible coupling with some wing or control surface mode. The 'lead-lag' mode (with displacements in the xy plane) have not been included, since the main preoccupation is the coupling between bending, torsion and aileron modes. Higher modes were disconsidered.

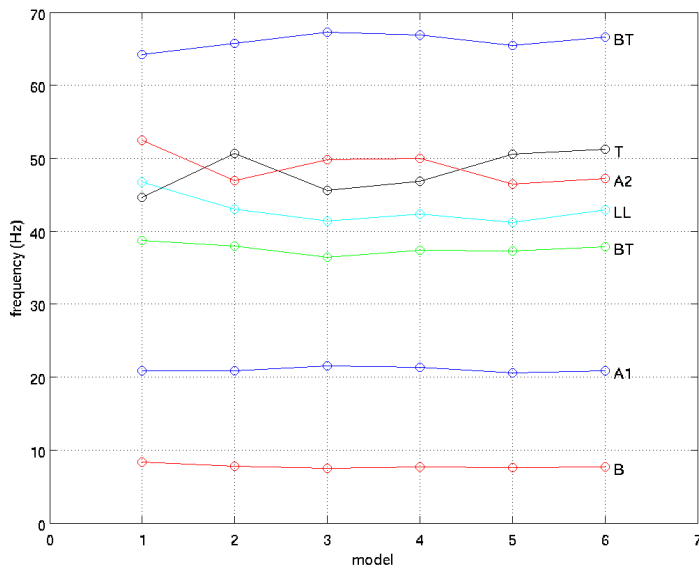
The aerodynamic model consists of 9 strips with two different properties: the inner 5 have only two degrees of freedom, and the elastic axis has been set to 50% of the semichord, constant for all strips; the outer 4 strips have an additional degree of freedom, representing the aileron, with the elastic axis also at 50% of the semichord, the leading edge of the aileron at

50% of the semichord, and its hinge line at 55%. These properties are predefined for the present analyzes. In the future, there will be an automatic calculation of the elastic axis based on the modal information.

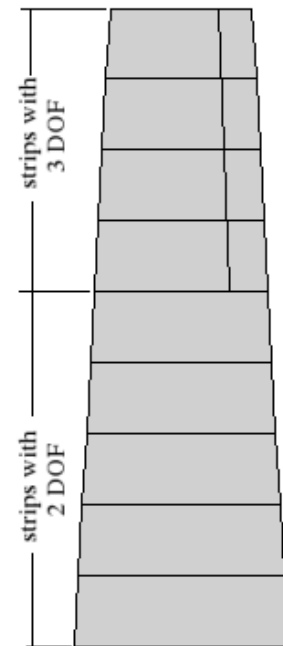
Table 3. List of wing structural normal modes with frequencies and mode identification for each lamination.

mode:	Model											
	f(Hz)	1	f(Hz)	2	f(Hz)	3	f(Hz)	4	f(Hz)	5	f(Hz)	6
1	8.35	B	7.80	B	7.45	B	7.66	B	7.58	B	7.69	B
2	20.84	A 1	20.88	A 1	21.58	A 1	21.34	A 1	20.55	A 1	20.89	A 1
3	38.77	BT	37.97	BT	36.39	BT	37.36	BT	37.29	BT	37.91	BT
4	44.60	T	43.06	LL	41.38	LL	42.39	LL	41.25	LL	42.95	LL
5	46.79	LL	46.98	A 2	45.57	T	46.88	T	46.48	A 2	47.26	A 2
6	52.44	A 2	50.66	T	49.79	A 2	49.98	A 2	50.55	T	51.23	T
7	64.22	BT	65.73	BT	67.25	BT	66.92	BT	65.51	BT	66.58	BT
8	79.95	BT	83.81	BT	79.20	BT	82.03	BT	83.61	BT	84.93	BT
9	86.76	x	91.03	x	93.10	x	93.32	x	91.14	x	91.63	x
10	88.83	x	95.28	x	96.31	x	96.14	x	95.69	x	95.20	x

B = bending; T = torsion; A = aileron mode; TB = torsion /bending mode; LL = lead-lag.



(a) Frequencies behavior for each model (from 1 to 6).



(b) Wing aerodynamic model.

Figure 3. Wing aerodynamic model.

4. NUMERICAL RESULTS

The flutter analysis were performed using a code written in MATLAB, with the structural information given by the files '.bdf' and '.f06' from the NASTRAN FEM analysis model. These files are read and the modal space structural model is then processed inside the code. Since a complex structural model will have a excessive number of nodes, and consequently, a high number of degrees of freedom, it is necessary to reduce the model order. This is done by a selection of representative points, as introduced in section 2. In Fig. 2, in previous section, the selected points to characterize the modes considered in the present aeroelastic analysis are shown.

A reduced frequency range must be set to compute aerodynamic influence coefficients matrices using Roger's approximation. This range is calculated based on the natural modes frequencies and on the desired velocities, as a first approach.

For $b = 1.25$, velocity values between 1 m/s and 250 m/s, and normal frequencies between 7 Hz and 90 Hz, the range of reduced frequency is 0.9 to 35.0. However, a series of runs showed that with a maximum value of 5.0 a converged solution is obtained.

The number of lag terms is also important for the calculations. It adjust the polynomial terms to be used in the Padé's interpolation. The definition of the number of terms depends on the problem: an excessive number of terms increases the size of matrices, and the computational effort; an lower number decreases the method accuracy. A compromise solution must be found for the definition of values and ranges.

Once the state space aeroelastic matrix is assembled, eigenvalues and eigenvectors representing the eigensolution for stability analysis are computed. From the complex eigenvalues it is possible to compute the damped natural frequencies. Flutter evolution curves, also known as 'vgf' curves, are presented in Figures 4(a) to 6(b). This type of curve is a similar way to plot the root locus, where the flow speed instead the gain is plotted along the abscissa axis.

The models under investigation were divided in pairs, with specific differences between each pair (see Tab. 2). The results are discussed here for pairs 1 and 2, 3 and 4, 5 and 6. The influence of lamination parameters in the vgf/curves is clear, with many differences between wings with same weight, geometric parameters and aileron torsional stiffness.

In Fig. 4(a) the result for model 1 is presented. This is a reference model, with all layers lined up in the spanwise direction. This kind of construction lead to a flexible wing, with a strong flutter condition being indicated by the coalescence between the second aileron mode and the first bending-torsion mode. As can be seen in figure 4(b), the inclusion of 2 layers at 45° increase the stiffness in the spanwise direction, what modifies the bending-torsion mode, avoiding the strong coalescence with the aileron mode.

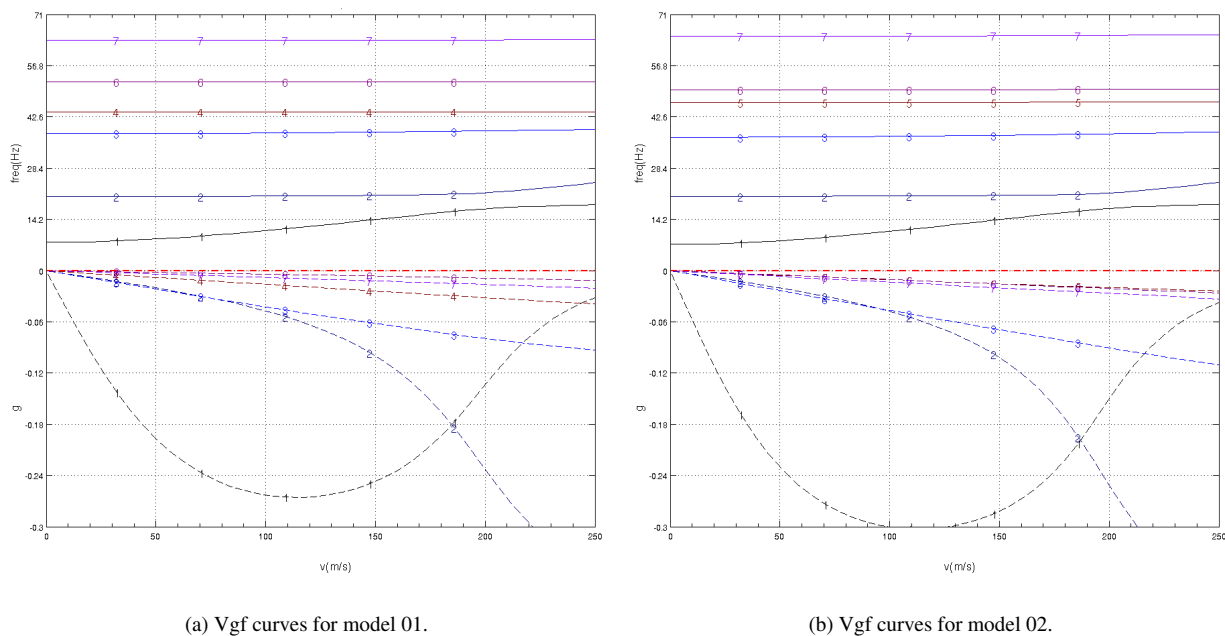
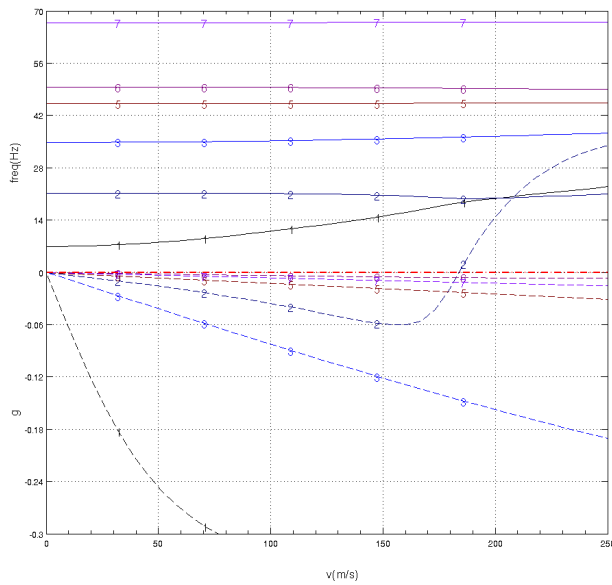


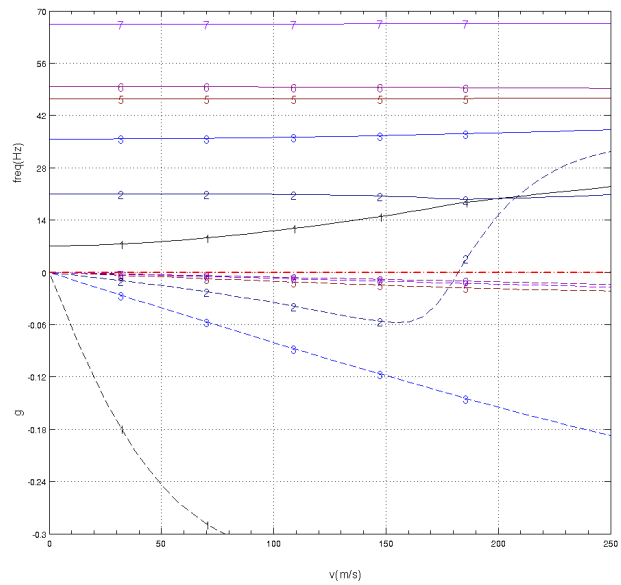
Figure 4.

In Fig.5 below, the results for models 03 and 04 are presented. These models have a combination of layers at 0° , 45° and 90° . These are the most common stacking sequence in aeronautical construction, since these are the easiest way for lamination and for layer direction control. No relevant differences can be found between these two models, but they are essentially different from the previous ones, because of the inclusion of the 90° layers. The differences are due to higher stiffness in the chordwise direction introduced by these new layers. The most important result is the presence of a classical flutter curve in the damping side in both curves.

The curves 6(a) and 6(b) below show the results for models with layers at 30° . The idea was to verify the influence of small modifications of orientation angles. This is not a common practice at the industry, due to the need of specific tools for a different alignment in the molding process. In these results, the most important differences arose from the suppression of the 90° layers again. A strong influence in the damping behaviour of first mode is noticed, and the torsion modes become again more effective, with effects in the second mode also noticeable. The flutter condition that appeared in previous modes is not present anymore.

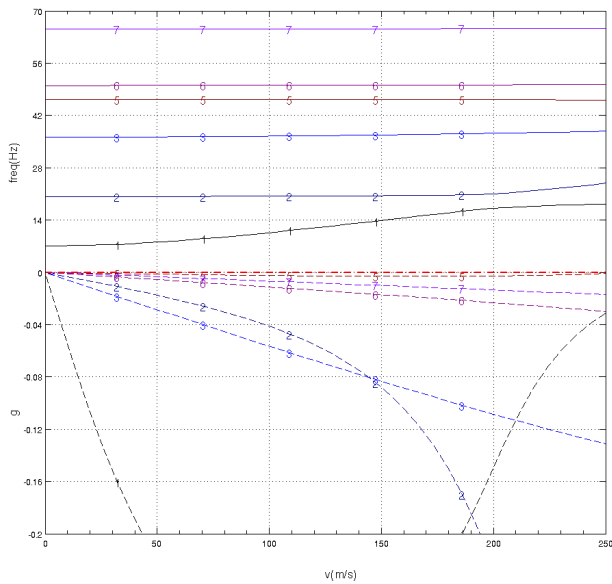


(a) Vgf curves for model 03.

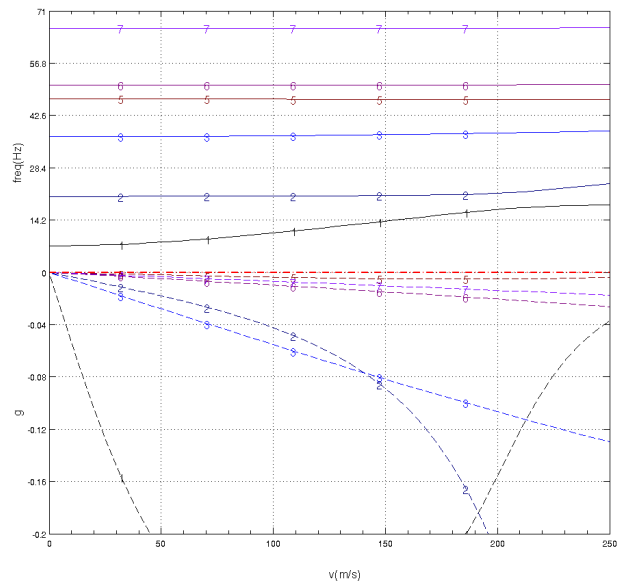


(b) Vgf curves for model 04.

Figure 5.



(a) Vgf curves for model 05.



(b) Vgf curves for model 06.

Figure 6.

5. CONCLUSION

The scope of the present investigation focuses the influence of ply orientation on wing flutter characteristics. It is a preliminary way to investigate aeroelastic tailoring. It could be noted the ply direction changes significantly the torsional stiffness characteristics. This behavior was clearly observed when comparing the aeroelastic modal evolution curves of model 1 and model 2. In the former case a 90 degree oriented layer was introduced, and the aeroelastic coupling mechanism was diffculted. This is so because stiffness orientation changes can represent a constrain for coupling mechanism. Furthermore, not only stiffness orientation, but probably the resulting elastic axis was modified.

The results obtained are promising for the continuation of the work. It is necessary to address better the interpolation of structural model points to the aerodynamic points, because this is the procedure that gives the modal information to the normalization procedure. The main concern are the degrees of freedom associated to control surfaces.

The next steps include the design and construction of scaled models for wind-tunnel experiments. They will allow the adjustment of computational model parameters and implementation of analysis methods, and, moreover, will serve as benchmark models for investigation of aeroelastic tailoring.

6. ACKNOWLEDGEMENTS

The authors would like to acknowledge the support of CNPq through a grant for the *Programa de Iniciação Científica*.

7. REFERENCES

- Maher N. Bismarck-Nasr. *Structural Dynamics in Aeronautical Engineering*. 1999.
- Carlos E. S. Cesnik, Dewey H. Hodges, and Mayuresh J. Patil. Aeroelastic analysis of composite wings. In AIAA, editor, *Structural Dynamics and Materials Conference and Exhibit*, number AIAA-96-1444-CP. AIAA, 1996.
- W. F. da Rocha. Determinação da velocidade de instabilidade aeroelástica de asa retangulares constituídas de material compósito em regime de voo subsônico. Trabalho de graduação, ITA, Campo Montenegro, São José dos Campos, SP, Brasil, 1999.
- R. G. A. da Silva. Análise aeroelástica no espaço de estados aplicada a aeronaves de asa fixa. Master's thesis, Escola de Engenharia de São Carlos, USP, 1994.
- J. Duchon. *Constructive Theory of Functions of Several Variables*, chapter Splines Minimizing rotation-Invariant Semi-Norms in Sobolev Spaces, pages 85–100. Springer, 1976.
- R. L. Harder and R. N. Desmarais. Interpolation using surface splines. *Journal of Aircraft*, 9:189–191, 1972.
- H.J. Hassig. An approximate true damping solution of the flutter equation by determinant iteration. *J. Aircraft*, 8, 1971.
- R.M. Jones. *Mechanics of Composite Materials*. Scripta Book Company, Washington, second edition edition, 1999.
- MSC. Quick reference guide. Technical report, The MacNeal-Schwendler Corporation, 2001.
- J.N. Reddy. *Mechanics of Laminated Composite Plates: theory and analysis*. CRC Press, Boca Raton, FL, 1997.
- L.W. Rehfield. Use of grid-stiffened structures for aeroelastic tailoring of wing. In Fu-Kung Chang, editor, *Tenth US-Japan Conference on Composite Materials*. American Society for Composites, 2002.
- K.L. Roger. Airplane math modeling methods for active control design. Technical Report AGARD-CP-228, AGARD, august 1977.
- M. Shirk, T. Hertz, and T. Weisshaar. Aeroelastic tailoring - theory, practice and promise. *J. Aircraft*, 23(1):6–18, 1986.
- R. Vepa. Finite state modeling of aeroelastic system. Technical Report NASA-CR-2779, NASA, February 1977.
- ZONA Technology, editor. *ZAERO Theoretical Manual*. Version 8.0. ZONA Tech., 2007.

8. Responsibility notice

The authors are the only responsible for the printed material included in this paper